processes

Article

Effect of Shear Flow on Drag Reducer Performance and Its Microscopic Working Mechanism

Zhiyu Liu [1], Zaifu Tian [2], Haoren Yuan [2], Yuan Li [1], Hongkui Ge [1,*] and Fujian Zhou [1,*]

1 State Key Laboratory of Petroleum Resources and Engineering, China University of Petroleum, Beijing 102249, China; zhiyuliu@cup.edu.cn (Z.L.); 2017310210@student.cup.eud.cn (Y.L.)
2 Oil Production Technology Research Institute, Shengli Oilfield Luming, China Petrochemical Corporation (Sinopec Group), Dongying 257000, China; giraffe8868@163.com (Z.T.); yuanhr1981@126.com (H.Y.)
* Correspondence: lzy8863766@163.com (H.G.); zhoufj@cup.edu.cn (F.Z.)

Abstract: As the development of unconventional oil and gas resources goes deeper, the stimulation of reservoirs goes deeper year by year. Flow in longer wellbores poses a challenge to the stability of drag-reduction performance of fracturing fluid. However, at present we have limited understanding of the mechanism of drag-reduction damage caused by shear flow, especially the microscopic mechanism. Therefore, in this work, the variation pattern of drag reducer solution performance with shear rate has been analyzed by using a high precision loop flow drag test system. The test results show that there is a critical shear rate for the performance damage of the drag reducer solution, and high strength shear flow and cumulative shear flow time are the main factors leading to the performance degeneration of the drag reducer. Based on the nanometer granularity distributions, rheological properties and microscopic structures observed with a transmission electron microscope of drag reducer solutions subjected to shear flows of different velocities, it is confirmed that the damage to the microscopic structure of the solution is the main reason leading to its performance degeneration. The destruction of the microscopic structure causes the drag reducer solution to degrade in non-Newtonian characteristics, so it becomes poorer in its capability of reducing turbulent dissipation and drops in drag-reduction capability. This research can provide a reference for improving and optimizing drag-reduction capability of fracturing fluid.

Keywords: drag reducer for slick water fracturing fluid; shear failure; grain size distribution; rheological properties; micro-mechanism of shear failure

Citation: Liu, Z.; Tian, Z.; Yuan, H.; Li, Y.; Ge, H.; Zhou, F. Effect of Shear Flow on Drag Reducer Performance and Its Microscopic Working Mechanism. *Processes* **2022**, *10*, 1485. https://doi.org/10.3390/pr10081485

Academic Editors: Linhua Pan, Minghui Li, Lufeng Zhang, Jie Wang, Wei Feng and Yushi Zou

Received: 13 July 2022
Accepted: 24 July 2022
Published: 28 July 2022

1. Introduction

Drag reducers are a kind of key additive in fracturing fluid for large scale hydraulic fracturing [1], which can reduce the friction of fracturing fluid flowing from ground surfaces to reservoirs effectively. As reservoirs developed become deeper year by year, the performance degeneration of drag reducers caused by flow shear degradation during flow has been becoming worse [2]. Currently, drag reducers commonly used are polymer type [3], so examining the variation patterns of polymer drag reducer performance caused by shear flow, the working mechanism and control mechanism of shear flow degradation is of great significance for improving the stability of drag reducer and fracturing effect.

The drag-reduction phenomenon is also called TOMs; that is, the addition of a small amount of polymer into water can reduce the flow resistance of water significantly [4,5]. Drag-reduction performance is affected by a number of factors. The degeneration of drag-reduction performance caused by mechanical degradation has always been a focus of study [6]. Earlier studies are the basis of subsequent ones. A lot of studies have shown that in the course of mechanical degradation of polymer, there might be break in the polymer chain structure. Among them, Merril and Horn proved that turbulent flow could cause the polymer drag-reduction capability to degenerate through straight pipe flow experiments, and concluded that structure breaking happened mostly at the midpoints of large molecules [7,8]. On this basis, Odell found through experiments that when subjected to shear higher than a critical rate, isolated large molecules would drop to half of their original molecular weights [9–11]. Vanapalli et al. verified the theory that the break of large molecules at midpoints caused mechanical degradation of polymers by chromatographic analysis [12]. After a large number of physical experiments, Brostow et al. proposed a theoretical model of molecule degradation in turbulent flow, which fitted well with experimental data [13]. Kim et al. investigated mechanical degradation of polymer with a novel rotating disc device and found that the degradation degree of a solution was affected by the solubility of the solvent [14–16]. Shanshool et al. focused their study on the concentration of drag reducer and found that high concentration solutions were not susceptible to mechanical degradation [17,18]. Research that focused on empirical equations of mechanical degradation is represented by the studies of Hénautet (2012) and Pereira (2012) [19,20]. Studies on how to prevent mechanical degradation are represented by the one by Zadrazil et al., 2012 [21]. All these studies promoted the study of mechanical degradation of drag reducer solutions. In recent years, on the basis of previous research results, Edson J examined the variation patterns of drag reducer performance due to mechanical degradation with concentration, molecular weight, temperature, and Reynolds number [22,23]. By introducing the abrupt contractions method into their study, Ivanor M. et al. found the relationship between drag-reduction rate and molecular weight and proposed the corresponding drag-reduction model [24]. Mohamm M. et al. explored the variation patterns of viscoelastic properties of drag reducer solution when affected by mechanical degradation, and concluded that drag-reduction performance was not affected by the small amplitude of oscillatory shear, but was related to continuous tensile failure [25]. The above studies have provided references for and promoted the study of mechanical degradation of drag reducer solution.

In the process of reservoir stimulation fracturing, fracturing fluid with the drag reducer additive is often injected into the target formation to create the hydraulic fractures by fracturing pumping trucks with a high flow rate and high shear rate, which can significantly affect the drag-reduction efficiency performance. However, the effect of flow shear rate on drag-reduction efficiency of the drag reducer has rarely been investigated due to the lack of a fluid pipe flow device with high shear rates. The novelty of this work is to build a novel pipe flow device with a high shear rate to investigate the relationships between the drag-reduction rate of the drag reducer solution and the shear rate under different flow conditions. Moreover, the effects of shear rate on grain size of agglomerates and rheological properties of drag reducer solution were also analyzed. In addition, the SEM was conducted to investigate the effects of shear rate on the microstructure of the drag reducer.

In this work, the relationships between the drag-reduction rate of the drag reducer solution and the shear rate under different flow conditions were researched by pipe flow experiments. Our results show that shear degradation of the drag reducer occurs at the high flow shear rate stage. The SEM results demonstrated the relationship between the degeneration of drag-reduction performance and mechanical degradation of the polymer drag reducer. Concerning the mechanical element of drag-reduction degeneration, it is concluded that the destruction of net-like structure makes the polymer solution weaker in non-Newtonian fluid features (a drop in viscoelasticity), increases the turbulent dissipation, and causes deterioration in drag-reduction capability. This result will provide a useful reference for the field application of the drag reducer when it is injected during hydraulic fracturing. The results will provide construction guidance for pumping the temporary plugging agent and its fracturing fluid in the field, helping to avoid the risk of drag reducer degradation at high shear rates.

2. Experiment Apparatus and Materials

2.1. Experiment Apparatus

In the experiments, a Zetasizer Nano ZS was used to analyze the distributions of grain sizes of polymer agglomerates in the drag reducer solutions, a Hakke MARSIII rheometer was used to test the rheological properties of the drag reducer solutions, and a JEM-100 transmission electron microscope made by JEOL was used to observe the micro-structures of the drag reducer solutions. The drag-reduction tests of drag reducer solutions were carried out in a high precision loop flow drag test system. With this system, the drag-reduction performance of a solution under the effect of shear flow can be tested under the circulation of fluid. The loop flow drag test system, modified from the friction tester, consists of a fluid supply system, an experimental pipe system, a pressure test system, and a data collection system. The structure of the loop flow drag test system is shown in Figure 1.

Figure 1. Loop flow drag test system.

To improve the accuracy of drag-reduction rate test, the fluid supply system and power delivery unit of the friction test equipment were modified. The fluid supply system after modification is composed of 3 tanks, which are used to store the solution to be tested, the back-flow solution, and fresh water, separately, to eliminate the interference between tested fluids. The power delivery unit was modified into a screw pump with a maximum pumping rate of 2.5 m^3/h to effectively eliminate the shear failure in the polymer solution caused by the turbine pump. The flow drag test system can measure the drags of fresh water and drag reducer solution under the same flow conditions accurately, thus enhancing the precision of experimental measurements. The pipe system mainly consists of three stainless steel pipelines of 6 mm, 8 mm, and 10 mm in diameter, respectively, and 3 m in length each. To minimize the additional effect from the corners connected to each pipeline, pressure measuring points are set at 0.25 m away from both ends, so each pipeline has an effective test length of 2.5 m. Pressure drop in the pipeline is measured with the differential pressure transducer connected between two pressure test points. As the pipelines of different diameters may vary widely in flow drag pressure drop, two differential pressure transducers of different ranges, 5 MPa (0.5–5.0 MPa, $\pm$0.1 kPa) and 0.5 MPa (0–0.5 MPa, $\pm$0.02%), are installed. In actual tests, the differential pressure transducer that meets the measurement accuracy requirements can be switched according to the pressure drop in flow in the pipeline.

2.2. Experimental Materials

The drag reducer used in the experiments was a kind of anion polymer emulsion, DR-800, made by Shengli Petrochemical Company Ltd. (Zibo, China). The effective component of the drag reducer is polyacrylamide copolymer synthesized from a mixture of acrylamide (AM), acrylic acid (AA), 2-acrylamido-2-methylpropanesulfonic acid (AMPS), and butyl acrylate (BA) in aqueous solution by polymerization process. The drag reducer solution used in the experiments was 0.05% in volume concentration.

3. Experimental Principle and Method

3.1. Experimental Principle

Drag reducer solution can make the flow resistance of fluid drop significantly when entering the flow pipe. This is shown as an increase in pumping rate and decrease in the friction pressure drop in the fluid. When the fluid in the pipe is pumped at a constant pressure, the effect of drag reduction is shown as increase in the fluid flow rate; when the fluid is pumped at a constant flow rate, the effect of drag reduction is shown as a decrease in friction pressure drop.

To better characterize this physical phenomenon, drag-reduction rate was introduced to evaluate the drag-reduction performance of the drag reducer solution. The drag-reduction rate (*DR*) is the most significant physical parameter in the present study; it is the physical parameter used to estimate the drag-reduction degree in the different shear rates of flow. As the drop in flow resistance of the fluid in the pipe is the result of the decrease in the flow friction coefficient in essence, the drag-reduction rate is defined as the reduction rate of the friction coefficient:

$$DR\% = \frac{\lambda_0 - \lambda_{DR}}{\lambda_0} \times 100\% \tag{1}$$

where:

$DR\%$—Drag-reduction rate;

λ_0—Friction coefficient of fresh water with no drag reducer added;

λ_{DR}—Friction coefficient of drag reducer solution.

In the experiments, it is difficult to measure the friction coefficient directly, so concerning the general formula of flow resistance in the straight pipe, the Fanning equation is adopted:

$$\lambda = \frac{2D}{\rho u^2 L}\Delta P \tag{2}$$

where:

D—Inner diameter of the pipe, m;

P—Fluid density, kg/m^3;

u—Flow velocity of the fluid, m/s;

L—Pipe length, m;

ΔP—Friction pressure drop in the fluid, Pa.

For experiments in the same pipe, both D and L are constant values. Meanwhile, as the amount of drag reducer added is very small, the density variation of the fluid after addition of the drag reducer is negligible. Therefore, under the same flow parameter (average flow velocity) of the fluid, the relation between the drag-reduction rate and the friction pressure drop in the pipe can be obtained by substituting Equation (2) into Equation (1):

$$DR\% = \frac{\Delta P_0 - \Delta P_{DR}}{\Delta P_0} \times 100\% \tag{3}$$

Hence, based on Equation (3), the friction pressure drops of the fluids with and without the drag reducer at two ends of the experiment pipe at the same flow velocity can be measured by differential pressure gauge, and then the drag-reduction rate of the drag reducer solution can be worked out by using the measured friction pressure drops.

In the experiments, mass flowmeter was used to measure the average flow velocity of fluid in the pipe. As the experiments aimed to find out the relationship between drag-reduction rate and shear rate of fluid flow, the relation between flow velocity and shear rate of fluid flow under a certain pumping rate was needed to calculate the corresponding shear rate of fluid flow. The formula for calculating shear rate of fluid flow was:

$$\gamma = \frac{4Q}{\pi R^3} = \frac{8u}{D} \tag{4}$$

where γ is the shear rate near the pipe wall, s^{-1}. As the shear failure of the fluid flow mainly concentrates near the pipe wall, this value is used to characterize the shear rate of the fluid flow. Based on the above principle, with the flow velocity of fluid regulated by the mass flowmeter, the friction pressure drops in fresh water and drag reducer solution and the flow velocity were measured, and then the relationship between drag-reduction rate and shear rate of fluid flow was worked out.

3.2. Experimental Method

3.2.1. Effect of Flow Shear on Drag-Reduction Performance of Drag Reducer

The loop flow drag test system was used to test the variation pattern of drag-reduction performance of the drag reducer solution with shear rate of fluid flow. A 30 L amount of the drag reducer solution at 0.05% concentration was prepared in the tank and blended evenly. By changing the pumping rate of the screw pump, pressure drops of the fluid in the pipe at different shear rates of fluid flow were measured. Then, the drag-reduction rates at different shear rates were calculated by using the pressure drop data to find out the variation pattern of drag-reduction rate with shear rate of fluid flow. Specifically, in the experiments, a frequency changer was used to change the pumping rate to make the shear rate of fluid flow in the pipe rise at a specific step length to the set value and then fall at the same step length, and this flow process was repeated several times. The effects of shear rate of fluid flow and cumulative shear time on drag-reduction performance of the drag reducer solution were analyzed based on the data obtained from the above experiments. To further analyze the effect of shear rate of fluid flow on drag-reduction performance, the drag reducer solution of the same concentration was prepared anew, with the maximum shear rate of fluid flow set at 2900 s^{-1} and 3500 s^{-1}, respectively; variation patterns of drag-reduction rate with shear rates of fluid flow were tested in different ranges of shear rates.

3.2.2. Effects of Flow Shear on Grain Size and Rheological Properties of Drag Reducer Solution

To find out the effect of fluid shear rate on agglomerate grain size and rheological properties of drag reducer solution, samples of drag reducer solution not subjected to shearing, drag reducer solution subjected to repeated low-rate shearing, and drag reducer solution subjected to repeated high-rate shearing were taken and coded as A, B, and C, respectively. Then, Zetasizer Nano ZS was used to obtain the grain size distributions of agglomerates in these samples. Finally, Hakke MARSIII rheometer was used to analyze the rheological characteristic curves of the three samples to find the relationship between agglomerate grain size and rheological behavior.

3.2.3. Effect of Flow Shear on Micro-Structure of the Drag Reducer Solution

The three samples were observed with a JEM-100CX transmission electron microscope made by JEOL. In the observations, the amplifications were kept the same as far as possible to compare the micro-structures of the polymers subjected to flow shear of different rates.

4. Results and Discussion

4.1. Effect of Flow Shear on Drag-Reduction Performance

The drag-reduction rates at different shear rates of flow were tested. The curve of the drag-reduction rate with shear rate (from 1000 s^{-1} to 6000 s^{-1}) of the 0.05% volume concentration drag reducer solution is shown in Figure 2.

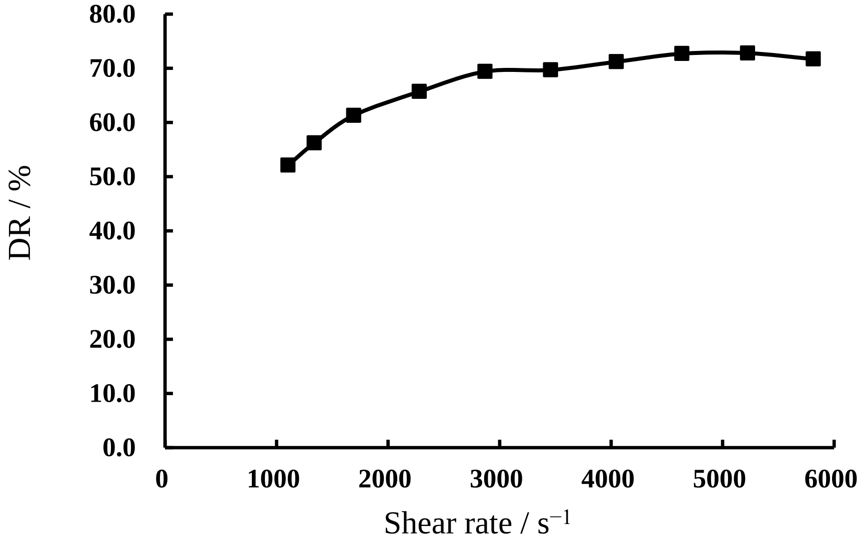

Figure 2. Relationship curve of drag-reduction rate with shear rate.

It can be seen from Figure 2 that with the gradual rise of shear rate the drag-reduction rate goes up gradually at first, but when the shear rate exceeds a critical value, the drag-reduction rate increases slowly and then even decreases. From this curve, an optimum drag-reduction rate can be found in the process of shear rate variations.

To verify this regularity, the drag-reduction rates of the drag reducer solution when the shear rate dropped from 6000 s^{-1} to 1000 s^{-1} (at the same variation interval when the shear rate rose) were tested. The tested results are plotted in the same chart of Figure 2 to enable a comparison, as shown in Figure 3.

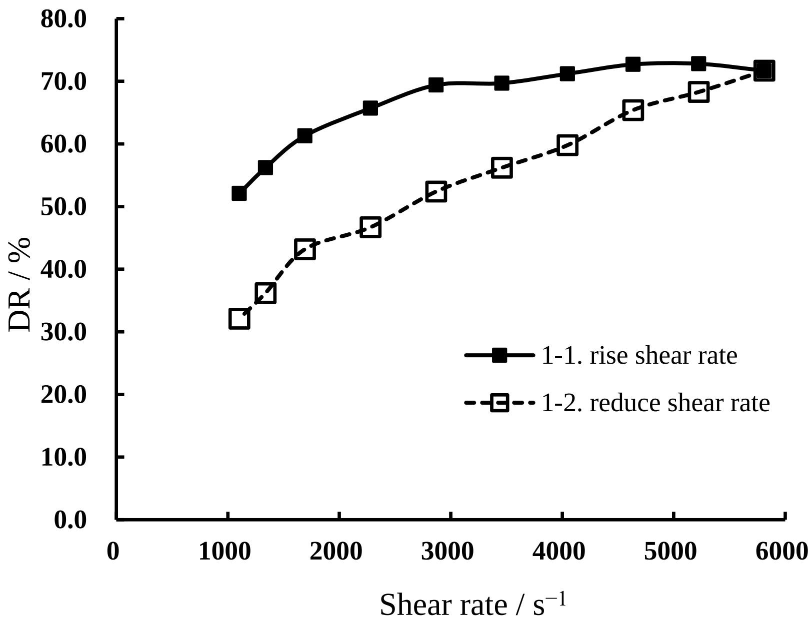

Figure 3. Curve of drag-reduction rate with rise and fall (at the same variation interval) of shear rate.

It can be seen from Figure 3 that the drag-reduction rate dropped significantly with flow shear, but the drag-reduction rate dropped different degrees at different shear rates. The curve shows large values in the left and smaller values in the right, indicating that the significant drop in drag-reduction rate appeared in the flow stages of the middle and left parts of the curve, while the drop in drag-reduction rate in the right side flow stage was small. This is because the long duration and the high rate of shear have a larger impact on the performance of the drag reducer solution and can lead to a considerable decrease in drag-reduction rate. However, when the cumulative shear flow time is short, the failure is not noticeable either. That is why the drag-reduction rate only dropped 6.4% at the shear rate of 5224 s^{-1}, while that at the shear rate of 1103 s^{-1} it dropped 35.3%; in other words, at the shear rate of 1103 s^{-1}, the drag reducer solution had experienced the whole shear process fortwo times longer than the process rise to the shear rate of 5224 s^{-1}, so the drag-reduction rate at this point dropped more significantly.

To verify this finding further, we repeated the flow experiment another three times. The shear rate in the four experiments varied in the same pattern and step length. The drag-reduction rates measured in the four experiments were plotted in the same chart (Figure 4).

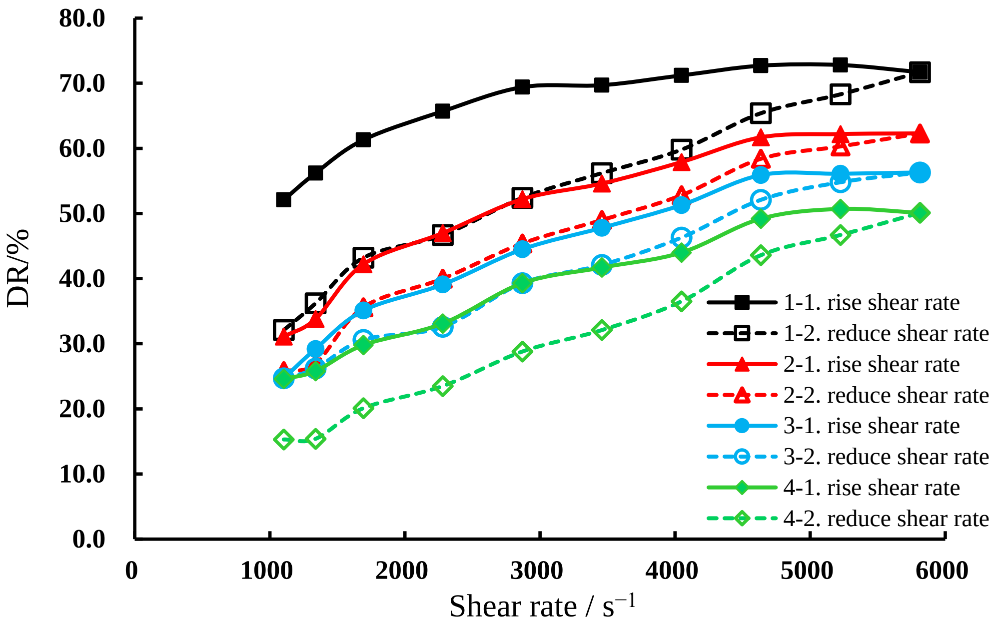

Figure 4. Variations of drag-reduction rate with shear rate from repeated experiments.

In Figure 4, curves of the same color represent the shear flow processes of rate rise and fall, respectively, in the same experiment; solid curves represent the process with shear rate rising gradually, and dotted lines represent the process with shear rate falling gradually. The curves from top to bottom show the drag-reduction rates measured in the first to fourth experiments, respectively. Comparison of the four groups of curves shows that each group of curves shows a variation pattern in drag-reduction rate similar to that mentioned above. Meanwhile, at high shear rate (5224 s^{-1}), all of them show a drop in drag-reduction rate of different degrees (3–10%). In particular, it is noted that the drag-reduction rate curve in the first shear rate decrease process almost coincides with that in the second shear rate increase process (the black dotted line and the red solid line sections at the shear rates between 1000 s^{-1} and 2900 s^{-1}). This means the performance of the drag reducer solution did not change much in this flow stage; in other words, the drag-reduction rate did not change much. Moreover, in the other repeated experiments, the relationship curves between shear rate and drag-reduction rate show similar features in the same flow stage. The drag reducer solution in this flow stage had experienced the nth time of high-rate shear, but did not experience the n + 1th time of high-rate shear. The coincidence of the two drag-reduction rate curves indicates that flow at low shear rates (less than 2900 s^{-1}) has little effect on the performance of the drag reducer. To sum up, high-rate shear may be the major factor leading to the degeneration of drag reducer performance; moreover, there is a critical value for the flow shear rate; only when the flow shear rate exceeds this critical value will the performance of the drag reducer be affected significantly. At flow shear rates over this critical value, longer cumulative shear time will make the performance of the drag reducer deteriorate further. To validate this finding, flow experiments at low flow shear rate (less than 2900 s^{-1}) and high flow shear rate (less than 3500 s^{-1} at maximum) were carried out. The experiments took the same shear rate variation pattern in the above experiments and were each repeated four times. To make the comparison of the experimental results easy, the drag-reduction curves were plotted with the method same as that of Figure 4.

4.1.1. Effect of Low-Rate Shear Flow on the Performance of Drag Reducer Solution

The variation pattern of the drag-reduction rate at low shear rate (less than 2900 s^{-1}) was further examined. The drag reducer solution at the volume concentration of 0.05% was prepared anew, and the same experiment method as that mentioned above was used. However, in this experiment, the maximum shear rate of flow was limited below 2869 s^{-1}, and the drag-reduction rate curves after four iterations of repeated shear flow are shown in Figure 5.

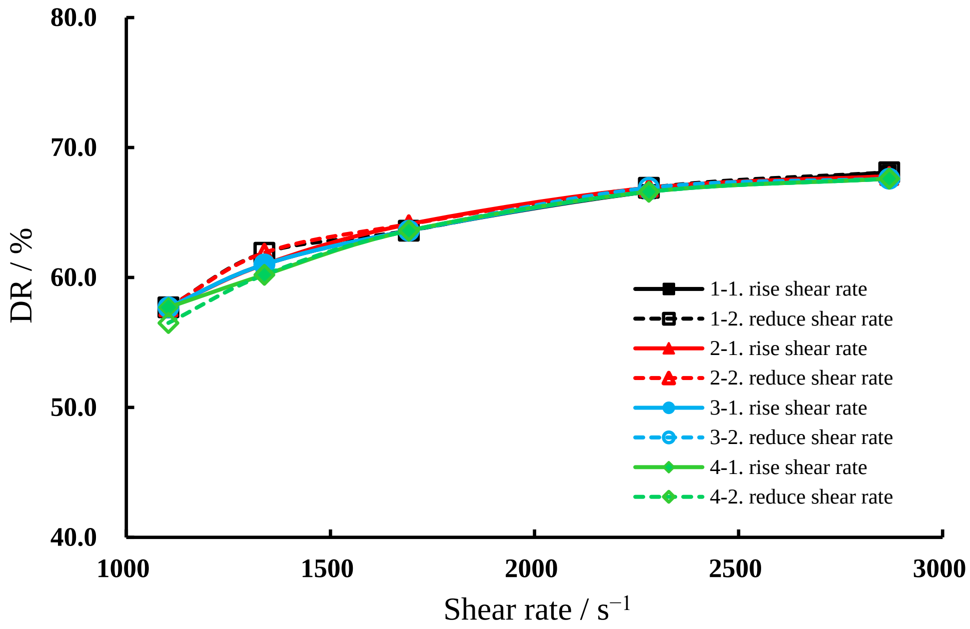

Figure 5. Variations of drag-reduction rate with low shear rate (controlled below 2900 s^{-1}).

Figure 5 shows shear rates below 2869 s^{-1}, the drag-reduction rate curves of the four repeated experiments basically coincide, and the drag-reduction rate variation at the same shear rate is only 1.5% at most. This means that with the maximum shear rate limited below 2900 s^{-1}, the drag reducer solution after four iterations of shear flow in the pipe caused little deterioration in drag-reduction performance.

4.1.2. Effect of High Shear Rate Flow on Performance of the Drag Reducer Solution

In this section, the variation pattern of drag-reduction rate at high shear rate of flow (3500 s^{-1} at maximum) was analyzed. Similarly, the drag reducer solution of 0.05% volume concentration was prepared anew, and the same experiment method as mentioned above was used. However, in this experiment, the maximum shear rate of flow was limited to 3458 s^{-1}, and the drag-reduction rate curves of four iterations of repeated shear flow are shown in Figure 6.

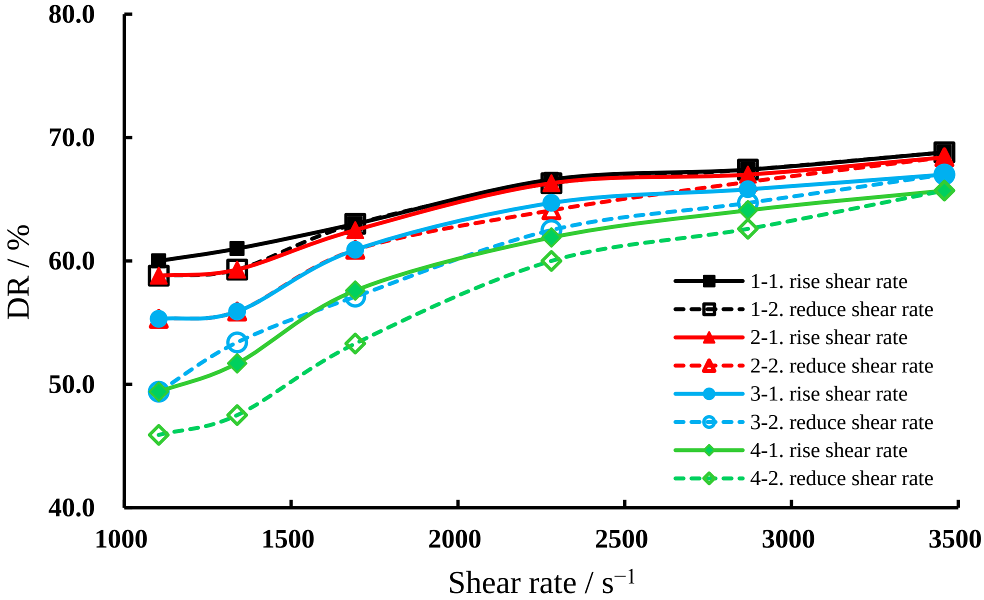

Figure 6. Curves of drag-reduction rate with shear rate (controlled below 3500 s^{-1}).

Figure 6 shows that with maximum shear rate was limited to 3458 s^{-1}; the drag-reduction rate varies in its pattern similar to that in the first flow experiment. The drag-reduction rates tested after four iterations of shear flow dropped significantly in comparison with thefirst test. In particular, at the shear rate of 1103 s^{-1} (the black solid line and green dotted line in this figure), the drag-reduction rate dropped by 23.5%. That is to say the drag reducer solution caused significant degeneration in drag-reduction performance after being subjected to high-rate shear for certain iterations cumulatively.

According to the understanding of the drag-reduction mechanism from mainstream studies, it is believed that the specific structure of polymers in drag reducer solutions leads to the non-Newtonian behavior of the solutions, and in turn to drag reduction. Looking back at the flow experiments in this work, it is found that the stable polymer structure in the drag reducer solution is damaged after high shear rate flow, and only when the cumulative damage reaches a certain degree will the drag reducer solution become worse concerning drag-reduction performance. Moreover, the shear rate of flow has a critical value; only when the shear intensity exceeds this critical value will the structure of the drag reducer be damaged, leading to degeneration in the drag-reduction rate. If the shear rate does not reach the critical value, no matter how long the cumulative flow time, the drag reducer rate will not change much. To validate this conclusion, rheological experiments and micro-structure analysis were carried out to explore the matter more deeply.

4.2. Variation Patterns of Grain Sizes and Rheological Behavior of Drag Reducer Solution under Shear Flow

The laser nano-granularity analysis results of samples A, B, and C are shown in Figure 7.

Through analysis it can be seen that the sample A not subjected to flow shear had agglomerate sizes concentrated between 200 nm and 500 nm. With the increase in shear rate of flow, the peak sizes of grains in the solution gradually shifted toward the left of the axis; that is to say the sizes of the agglomerates in the solution decreased with the increase in shear rate. In comparison, the sample subjected to low-rate shear flow had a wider span of peak values of grain sizes, indicating that it was affected by shear flow, part of the agglomerates were broken into smaller agglomerates, but due to different degrees of effect, the agglomerates in the solution ranged between 70 nm and 250 nm in size; in other words, they were smaller in value but wider in span in peak size. The sample subjected to high-rate shear flow had smaller agglomerates in the range between 30 nm and 80 nm; that is to say, the agglomerates in the solution had smaller peak size values in a smaller range.

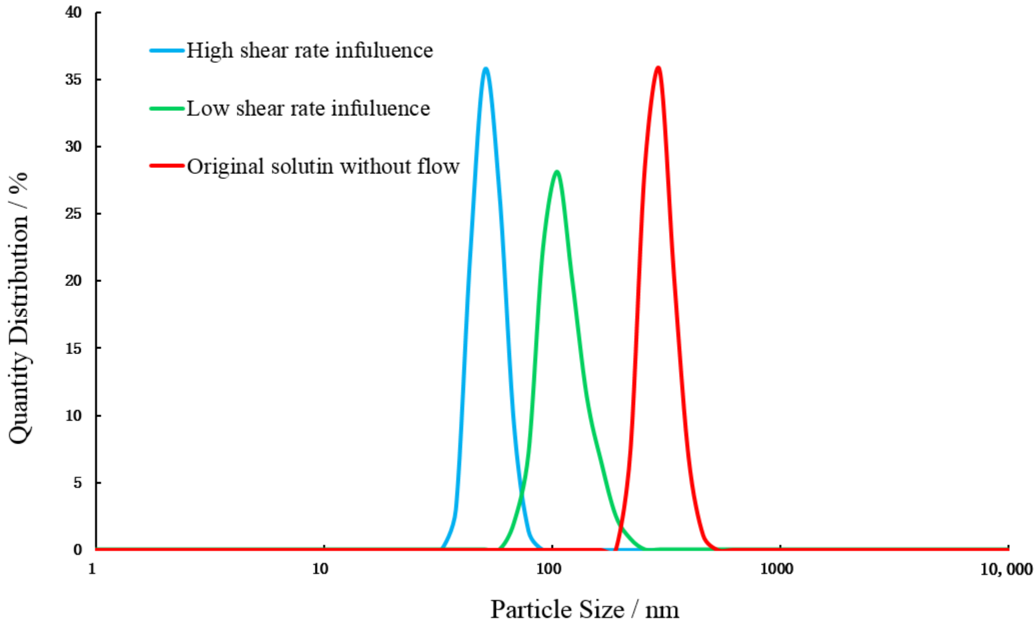

Figure 7. Distributions of grain sizes of the drag reducer solutions subjected to shears of different rates.

The rheological test results of the three samples are shown in Figure 8.

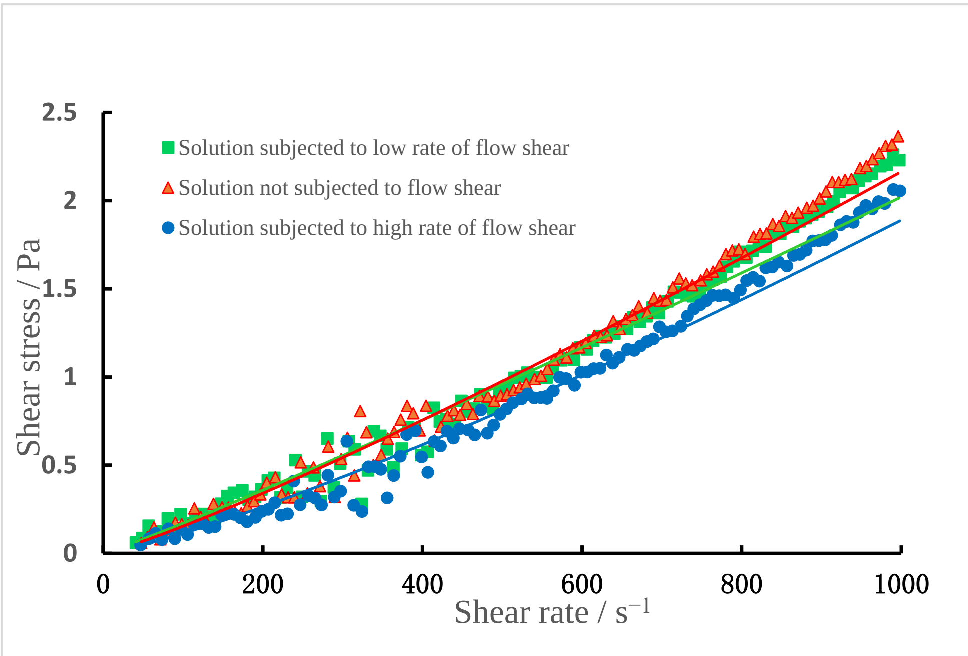

Figure 8. Rheological characteristic curves of the drag reducer solutions with shear rate.

By comparing the three curves of shear stress with shear rate, it is found that the three samples were similar in rheological behavior, all showing rheological features of power-law fluid (typical non-Newtonian fluid). When affected by shear flow, the drag reducer solution would turn weaker in power-law behavior and tend to be more like Newtonian fluid (fresh water). The more serious the shear failure of the solution, the weaker the non-Newtonian feature of the solution would be. Correspondingly, the solution decreased in viscosity and became weaker in viscoelasticity.

4.3. Variation Pattern of Micro-Structure of the Drag Reducer Solution

The micro-structure of the sample A not subjected to flow shear observed under electron microscope is shown in Figure 9.

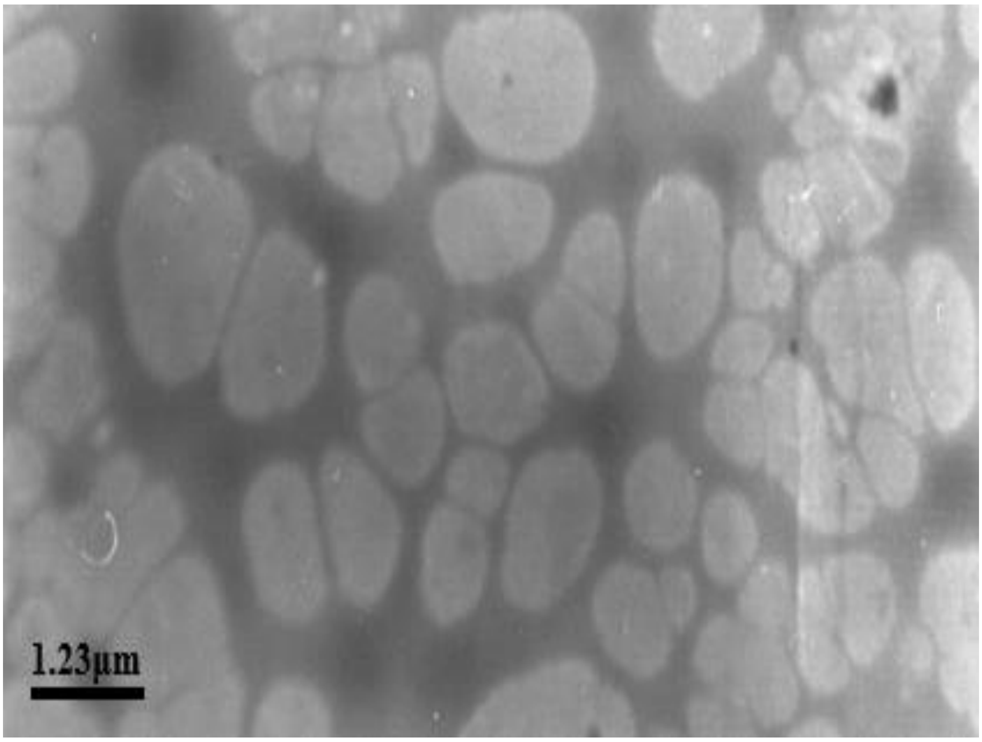

Figure 9. Micro-structure of the drag reducer not subjected to flow shear.

The darker parts in Figure 9 are polymer agglomerates observed. It can be seen from Figure 9 that most of the agglomerates were connected in a net-like structure, with obvious nodes observed. Some of the agglomerates were connected and extended into the mesh wall with a certain thickness, and the net-like structure was spread evenly in the solution. The stable agglomerate structure can improve the viscoelasticity of the drag reducer solution and reduce the turbulent dissipation during fluid flow effectively, thus lowering the flow friction.

The micro-structure of the sample B subjected to low-rate shear is shown in Figure 10.

It can be seen from Figure 10 that parts of the meshes were damaged, while the remaining parts of the meshes remained intact. The damaged meshes remained in the original distribution state but failed to form a complete wall structure and only the basic mesh shape remained. The drag reducer net-like structure in the solution changed in micro-structure after experiencing low shear rate flow. Although the main net-like structure remained, the wall of part of the meshes became thinner. Affected by shear stress of flow, the net-like structure was stretched, but as the shear rate of the flow was low, the shear stress did not destroy the net wall completely. Therefore, the drag reducer solution did not drop significantly concerning drag-reduction performance.

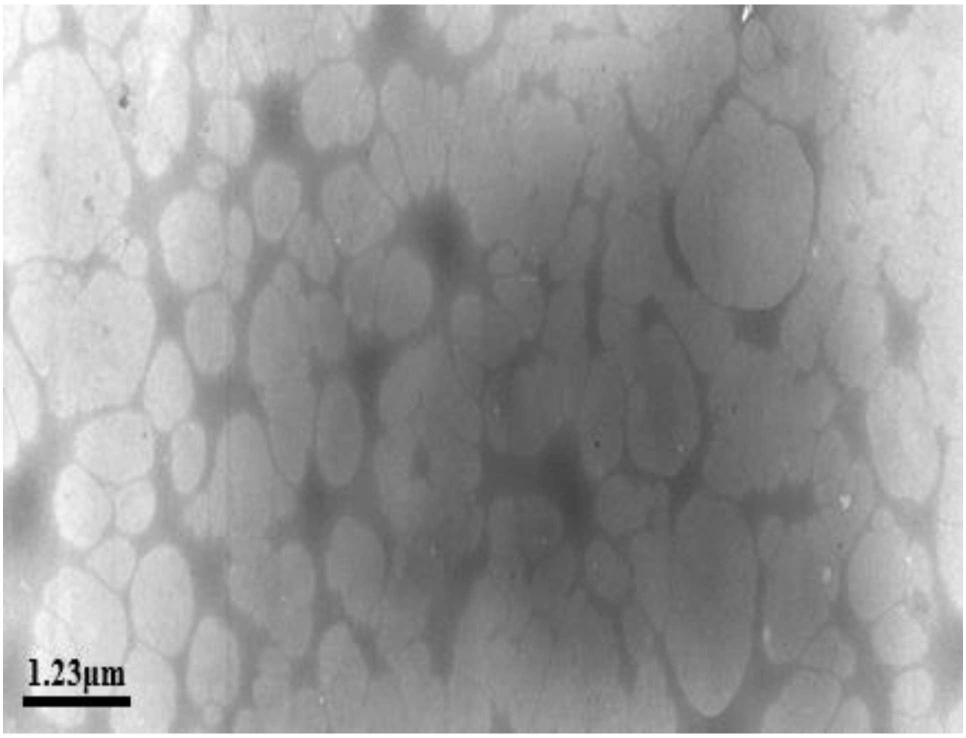

Figure 10. Micro-structure of the drag reducer after being subjected to low rate of flow shear.

The micro-structure of sample C experiencing high shear rate flow is shown in Figure 11, which is quite different from that of samples A and B.

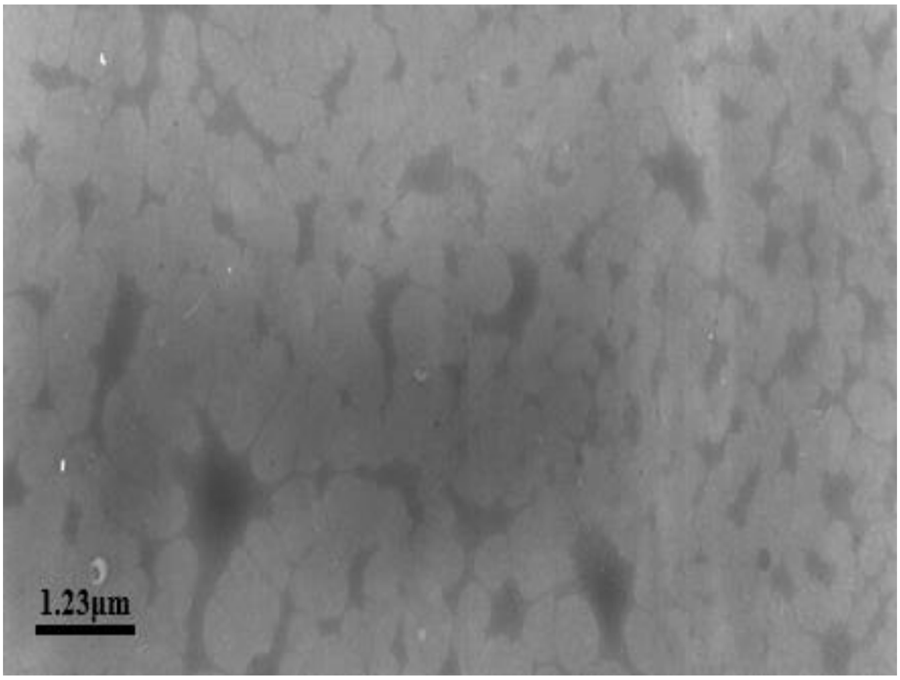

Figure 11. Micro-structure of the drag reducer after being subjected to high rate of flow shear.

It can be seen from Figure 11 that most of the net-like structure was destroyed, there were hardly any complete meshes, and most drag reducer agglomerates appeared in an isolated state. Moreover, the agglomerates were quite different in size and were distributed unevenly, and only a small number of nodes had an unstable structure connected by a small amount of stretched net-like structure.

In a word, from the above experiments of effect of flow shear rate on drag reducer micro-structure, it is concluded that the degeneration of drag-reduction performance of drag reducer solution is closely related to the destruction of the net-like structure of the drag reducer. The damage degree of the net-like structure of the drag reducer determines the degeneration degree of drag-reduction performance of the drag reducer solution, and the more severe the micro-structure damage, the more significant the drop in drag-reduction rate. However, after the damage reaches a certain degree (the net-like structure is completely destroyed), the drag-reduction rate tends to be stable again. The case in the low shear rate flow stage is different from that in the high shear rate flow stage. In the low shear rate flow stage, although the net-like structure is damaged to some degree, the enhancement of drag-reduction performance outweighs the negative effect of net-like structure stretch with the increase in flow velocity of the drag reducer solution. Moreover, part of the energy during structure stretching is stored in the drag reducer agglomerates, reducing the energy consumption, which is good for decreasing energy dissipation caused by turbulent flow. Therefore, in the initial stage, with the rise of flow velocity, the drag-reduction rate does not drop noticeably. However, even at low shear rate, a long time shear would result in damage the same as that of high shear rate flow, and finally the drag-reduction rate would become stable (that is, the drag-reduction rate after complete destruction of drag reducer structure).

5. Conclusions

In this work, the variation pattern of drag-reduction rate with shear rate was analyzed with a high precision loop drag test system. The reason why shear flow can influence the performance of the drag reducer was also explored. The distributions of grain sizes, rheological properties, and micro-structures of drag reducer solution samples were analyzed. On this basis, the mechanism of the high strength shear flow causing micro-structure damage, changes in rheological properties and degeneration of drag-reduction performance of the drag reducer solution were figured out. Through this research, the following conclusions have been reached:

1. With the increase in shear rate, the drag-reduction rate of the drag reducer solution will first rise to a peak value and then fall gradually. Then, with the increase in cumulative shear flow time, the drag-reduction rate will drop more significantly. Meanwhile, the shear rate causing drag-reduction drop has a critical value; only when the flow shear rate reaches this value will the performance of the drag reducer start to be damaged.
2. When subjected to flow shear higher than the critical rate, polymer agglomerates in the drag reducer solution will decrease in size. The higher the flow shear rate, the smaller the peak values of grain sizes and the higher the peak intensity of agglomerates in the solution.
3. The drag reducer solution shows typical characteristics of non-Newtonian fluid, which can be weakened by flow shear. The stronger the flow shear, the weaker the non-Newtonian fluid characteristics and the poorer the rheological behavior of the solution.
4. The damage of the net-like structure of the drag reducer is the main cause of degeneration of drag-reduction performance. Micro-mechanism research shows that the destruction of net-like structure caused by shear failure makes the polymer solution weaker in non-Newtonian fluid features (drop in viscoelasticity), leads to an increase in turbulent dissipation, and eventually results in the deterioration of drag-reduction capability.

Author Contributions: Conceptualization, H.G. and F.Z.; investigation, Z.T. and H.Y.; methodology, Z.L. and Y.L.; project administration, Z.L.; writing—original draft, Z.L.; writing—review and editing, Y.L. All authors have read and agreed to the published version of the manuscript.

Funding: This study is funding supported by Shengli Oil Field Luming Co., Ltd., "Research and application of temporary plugging technology in water fracture displacement of beach- bar sand reservoir water fracture displacement" (LMKJ2021-05), Xinjiang Deli Zhongcheng Petroleum Engineering Co., Ltd., "Research on new drag-reduction materials suitable for different fluid flow conditions" (ZC-20201209).

Data Availability Statement: The data presented in this study are available on request from the corresponding author.

Conflicts of Interest: The authors declare no conflict of interest.

References

1. Yang, B.; Zhao, J.; Mao, J.; Tan, H.; Zhang, Y.; Song, Z. Review of friction reducers used in slickwater fracturing fluids for shale gas reservoirs. *J. Nat. Gas Sci. Eng.* **2019**, *62*, 302–313. [CrossRef]
2. Muntasheri, A.; Critical, G.A. Review of Hydraulic Fracturing Fluids over the Last Decade. In Proceedings of the SPE Western North American and Rocky Mountain Joint Meeting, Denver, CO, USA, 17–18 April 2014.
3. Barati, R.; Liang, J. A Review of Fracturing Fluid Systems Used for Hydraulic Fracturing of Oil and Gas Wells. *J. Appl. Polym. Sci.* **2014**, *131*, 40735.
4. Toms, B.A. Some observations on the flow of linear polymer solutions through straight pipelines at large reynolds numbers. In Proceedings of the 1st International Congress on Rheology, Amsterdam, The Netherlands, 21–24 September 1948; Volume 2, pp. 135–141.
5. Toms, A. On the early experiments on drag reduction by polymers. *Phys. Fluids* **1977**, *3*, 20. [CrossRef]
6. Pereira, A.S.; Mompean, G.; Thompson, R.L.; Soares, E.J. Elliptical, parabolic, and hyperbolic exchanges of energy in drag reducing plane couette flows. *Phys. Fluids* **2017**, *29*, 115106. [CrossRef]
7. Horn, A.F.; Merrill, E.W. Midpoint scission of macromolecules in dilute solution in turbulent flow. *Nature* **1984**, *312*, 140–141. [CrossRef]
8. Merrill, E.W.; Horn, A.F. Scission of macromolecules in dilute solution: Extensional and turbulent flows. *Polym. Commun.* **1984**, *25*, 144–146.
9. Odell, J.A.; Muller, A.J.; Narh, K.A.; Keller, A. Degradation of polymer-solutions in extensional flows. *Macromolecules* **1990**, *2*, 23. [CrossRef]
10. Muller, A.J.; Odell, J.A.; Carrington, S. Degradation of semidilute polymer solutions in elongational flows. *Polymer* **1992**, *33*, 12. [CrossRef]
11. Nguyen, T.Q.; Kausch, H.H. Effects of solvent viscosity on polystyrene degradation in transient elongational flow. *Macromolecules* **1990**, *23*, 5137–5145. [CrossRef]
12. Vanapalli, S.A.; Ceccio, S.L.; Solomon, M.J. Universal scaling for polymer chain scission in turbulence. *Proc. Natl. Acad. Sci. USA* **2006**, *103*, 16660–16665. [CrossRef] [PubMed]
13. Brostow, W.; Ertepinar, H.; Singh, R.P. Flow of dilute polymer solutions chain conformations and degradation of drag reducers. *Macromolecule* **1990**, *23*, 5109–5118. [CrossRef]
14. Kim, C.A.; Kim, J.T.; Lee, K.; Choia, H.J.; Jhon, M.S. Mechanical degradation of dilute polymer solutions under turbulent flow. *Polymer* **2000**, *41*, 7611–7615. [CrossRef]
15. Kim, K.; Islam, M.T.; Shen, X.; Sirviente, A.I.; Solomon, M.J. Effect of macromolecular polymer structures on drag reduction in a turbulent channel flow. *Phys. Fluids* **2004**, *16*, 4150–4162. [CrossRef]
16. Kim, K.; Sirviente, A.I. Turbulence structure of polymer turbulent channel flow with and without macromolecular polymer structures. *Exp. Fluids* **2005**, *38*, 739–749. [CrossRef]
17. Shanshool, J.; Al-Qamaje, H.M.T. Effect of molecular weight on turbulent drag reduction with polyisobutylene. *NUCEJ Spatial.* **2008**, *11*, 52–59.
18. Shanshool, J.; Marwa, F.; Jabbar, A.; Sulaiman, I.N. The influence of mechanical effects on degradation of polyisobutylenes as drag reducing agents. *Pet. Coal* **2011**, *53*, 218–222.
19. Hénaut, I.; Glénat, P.; Cassar, C.; Gainville, M.; Hamdi, K.; Pagnier, P. Mechanical Degradation Kinetics of Polymeric DRAs. In Proceedings of the 8th North American Conference on Multiphase Technology, Banff, AB, Canada, 20–22 June 2012.
20. Pereira, A.S.; Soares, E.J. Polymer degradation of dilute solutions in turbulent drag reducing flows in a cylindrical double gap rheometer device. *J. Non-Newton. Fluid Mech.* **2012**, *9*, 179–180. [CrossRef]
21. Zadrazil, I.; Bismarck, A.; Hewitt, G.F.; Markides, C.N. Shear layers in the turbulent pipe flow of drag reducing polymer solutions. *Chem. Eng. Sci.* **2012**, *72*, 142–152. [CrossRef]
22. Edson, J.S. Review of mechanical degradation and de-aggregation of drag reducing polymers in turbulent flows. *J. Non-Newton. Fluid Mech.* **2020**, *276*, 104225.

23. Vincenzi, D.; Watanabe, T.; Ray, S.; Picardo, J. Polymer scission in turbulent flows. *J. Fluid Mech.* **2021**, *912*, A18. [CrossRef]
24. Martins, I.; Soares, E.J.; Siqueira, R.N. Mechanical scission of a flexible polymer (polyethylene oxide) under highly turbulent flows through abrupt contractions. *J. Non-Newton. Fluid Mech.* **2022**, *301*, 104740. [CrossRef]
25. Mohammadtabar, M.; Sanders, R.S.; Ghaemi, S. Viscoelastic properties of flexible and rigid polymers for turbulent drag reduction. *J. Non-Newton. Fluid Mech.* **2020**, *283*, 104347. [CrossRef]